MULTISTABILITY IN A SEMICONDUCTOR LASER SUBJECT TO OPTICAL FEEDBACK FROM A FABRY-PEROT FILTER

H. ERZGRÄBER

School of Engineering, Mathematics and Physical Sciences
University of Exeter
Exeter EX4 4AU, United Kingdom
E-mail: h.erzgraber@exeter.ac.uk

B. KRAUSKOPF

Department of Engineering Mathematics
University of Bristol
Bristol BS8 1TR, United Kingdom

We study the structure of the multistable continuous wave emission region of a semiconductor laser subject to coherent optical feedback from a Fabry-Perot filter. Key parameters organizing the degree of multistability are uncovered, and they include the feedback phase and the frequency detuning.

Keywords: delay differential equation, optical feedback, bifurcation analysis

1. Introduction

Semiconductor lasers find many applications, for example, in optical telecommunication. Because of their high material gain they are very sensible to external perturbations, which may lead to instabilities and possibly even chaotic laser emission. We show here that this sensitivity can also lead to a complex structure of multistable continuous wave (cw) and oscillatory emission. More specifically, we consider a semiconductor laser that is subject to coherent optical feedback from a Fabry-Perot filter. Filtered optical feedback (FOF) is a frequently used set-up to control the dynamics of a laser via the spectral properties of the feedback light, which are determined by the filter detuning and the filter width. The system can be modelled by rate equations for the complex-valued laser field $E(t)$, the complex-valued filter field $F(t)$, and the real-valued laser inversion $N(t)$. In normalized

form [1,2] the model is given by,

$$\begin{aligned} \dot{E}(t) &= (1+i\alpha)E(t)N(t) + \kappa F(t)\,, \\ T\dot{N}(t) &= P - N(t) - (1+2N(t))|E(t)|^2\,, \\ \dot{F}(t) &= \Lambda E(t-\tau)e^{-iC_p} + (i\Delta - \Lambda)F(t)\,. \end{aligned} \tag{1}$$

This model takes into account the time delay τ of the feedback light that arises from the propagation through the feedback loop. Hence, the model Eqs. (1) takes the form of a system of delay differential equations; here time is rescaled with respect to the photon decay time, which is typically in the order of picoseconds. The laser parameters are the linewidth enhancement factor α, the ratio between electron and photon decay time T, and the pump parameter P. The feedback is characterized by the feedback strength κ, the feedback phase C_p, the linewidth of the filter Λ, and the detuning $\Delta = \Omega_F - \Omega_0$ of the filter from the laser; here Ω_F is the filter frequency and Ω_0 is the laser frequency. In accordance with experimental practice [3], we change the detuning in Eqs. (1) by changing Ω_0 while keeping Ω_F fixed. Importantly, the feedback phase C_p takes into account the phase that the laser field accumulates as it propagates through the feedback loop. The parameter were set to the realistic values that can be found in Table 1.

Equations (1) model the dynamics of a semiconductor laser subject to coherent optical feedback from a Fabry-Perot filter. Of particular interest in this system is the additional control over the feedback field in terms of the width Λ and the detuning Δ of the filter. Its dynamics has been studied experimentally and mathematically for example in Refs. [1–5]. In this system the laser receives maximum feedback intensity when its optical frequency equals the center frequency of the filter. An alternative operation of the filter, known as non-invasive feedback, has been studied, for example, in Refs. [6,7]; in this case the feedback intensity has its minimum when the laser operates at the center frequency of the filter.

A key observation is that Eqs. (1) have certain symmetries, and this has influence on the structure of its solutions. In particular, there is the S^1-symmetry

$$(E,\, F,\, N) \to (e^{i\varphi}E,\, e^{i\varphi}F,\, N)\,, \tag{2}$$

which corresponds to a rotation of the optical fields of the laser E and the filter F by an arbitrary angle $\varphi \in [0, 2\pi)$ in the complex plane. Moreover, there is the parameter symmetry

$$(E,\, F,\, N;\, C_p) \to (E,\, F,\, N;\, C_p + 2\pi)\,, \tag{3}$$

that involves the feedback phase C_p.

Table 1. Summary of the parameters and their normalized values.

Symbol	Meaning	Value
α	Linewidth enhancement parameter	5
T	Ratio between electron and photon decay time	100
P	Pump parameter	3.5
τ	Delay time	300
κ	Feedback strength	0.01
Λ	Linewidth of the Fabry-Perot filter (HWHM)	0.07
Ω_F	Center frequency of the Fabry-Perot filter	-0.07
Ω_0	Optical frequency of the laser	free
C_p	Feedback phase	free

2. External Filtered Modes

A continuous wave solution of system (1) characterizes a state where the FOF laser exhibits a constant intensity emission. It has the form

$$(E(t);\, N(t);\, F(t)) = (|E_s|e^{i\omega_s t};\, N_t;\, |F_s|e^{(i\omega_s t + i\phi)})\,, \tag{4}$$

where the laser field and the filter field oscillate with the same frequency ω_s and constant amplitudes $|E_s|$, $|F_s|$. There is a phase difference ϕ, and the laser inversion N_s is a constant. We call these solutions external filtered modes (EFMs) of the FOF laser. Mathematically, they correspond to group orbits of the S^1-symmetry Eq. (2) of the FOF laser system. In what follows, we analyse the stability of the EFMs as a function of the laser frequency Ω_0, which changes Δ in Eqs. (1), and as a function of the feedback phase C_p. A numerical bifurcation analysis with DDE-BIFTOOL [8] will reveal saddle-node (S) and Hopf (H) bifurcation curves that form the stability boundary of the EFMs as well as codimension-two points that indicate changes of the stability boundary.

3. Stability Analysis

Figure 1 shows the stability of the external filtered modes (EFMs) of the FOF laser system as a function of the laser frequency Ω_0. Stable EFMs are plotted thick and unstable EFMs are plotted thin; they change stability at saddle-node (+) and Hopf (∗) bifurcations. In a saddle-node bifurcation either a pair of EFMs collide and disappear, or new pair of EFMs is created. In a Hopf bifurcation an EFM looses stability and a periodic orbit is created; physically the laser intensity starts to oscillate. The EFMs (4) can be plotted in different representations. In particular, Fig. 1(a) shows the laser intensity $|E_S|^2$, which undergoes only relatively small variations

when Ω_0 is changed. Figure 1(b) shows the filter intensity $|F_s|^2$; it is large around $\Omega_0 = 0$, implying high feedback intensity. The filter intensity $|F_s|^2$ is close to zero for sufficient large and sufficient small laser frequency Ω_0. Figure 1(c) shows the actual frequency ω_s of the FOF laser system, which also varies as a function of Ω_0. Finally, Fig. 1(d) shows the phase Φ between the laser field E and the filter field F. For large and small values of Ω_0 the phase changes very rapidly as Ω_0 is varied. Only the part of the EFM

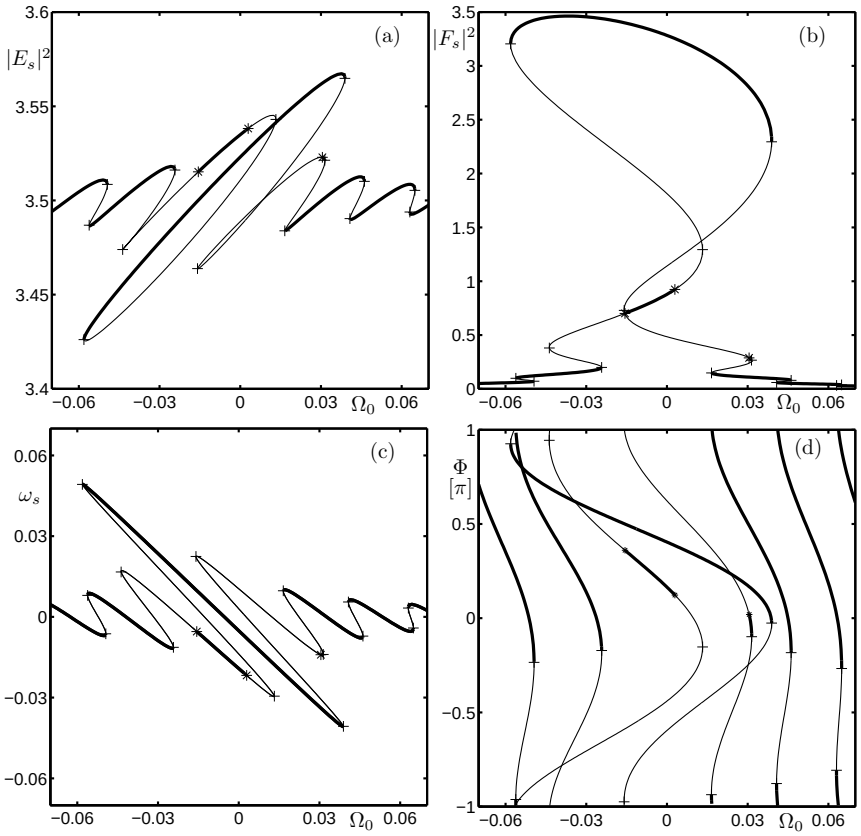

Fig. 1. One-parameter bifurcation analysis of the EFMs as a function of the laser frequency Ω_0. EFMs are stable along thick parts of curves and unstable along thin parts; also shown are saddle-node (+) and Hopf (∗) bifurcations. The individual panels show different representations of the same branch of EFMs: panel (a) shows the laser intensity $|E_s|^2$, panel (b) the feedback intensity $|F_s|^2$, panel (c) the FOF laser frequency ω_s, and panel (d) the phase shift Φ between the laser field and the filter field.

branch around $\Omega_0 = 0$, which corresponds to a high filter intensity $|F_s|^2$, exhibits less rapid variations. Indeed from Fig. 1 we can already identify several parameter intervals with bistable EFMs.

We now extend our stability analysis to two parameters by including the feedback phase C_p. Figure 2 shows a two-parameter bifurcation analysis in the (Ω_0, C_p) parameter plane. The stability regions of the EFMs are bounded by saddle-node (S) and Hopf (H) bifurcation curves; changes in the boundary are marked by codimension-two saddle-node Hopf (SH), Bogdanov-Takens (BT), and double Hopf (HH) points. Figure 2(a) shows the covering space of the 2π-periodic parameter C_p, where the gray shaded regions indicate stable EFMs. Because of the symmetry Eq. (3), each curve and region can be shifted by multiples of 2π. The result of this is shown in Fig. 2(b) where we now can restrict C_p to a fundamental 2π interval; for convenience we dropped the labeling. Since the 2π copies from Fig. 2(a) overlap each other we find multistable EFM regions. In particular, the white region indicates one stable EFM, the light gray region two stable EFMs, and the dark gray regions three stable EFMs.

As Fig. 2 shows, we find a considerable degree of multistability between different EFMs. In fact, changing other feedback parameters, such as the

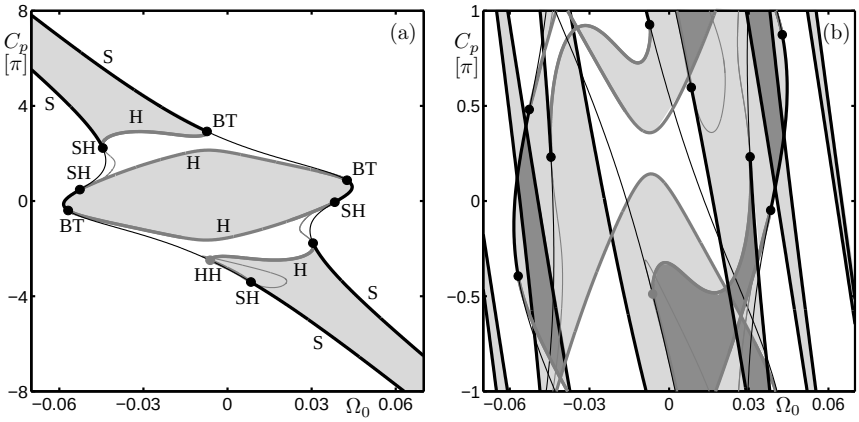

Fig. 2. Two-parameter bifurcation analysis of the EFMs in the (Ω_0, C_p)-plane. Shown are saddle-node (S) and Hopf (H) bifurcation curves; codimension-two points are saddle-node Hopf (SH), Bogdanov-Takens (BT) and double Hopf (HH). Panel (a) shows the covering space of the parameter C_p over several intervals of 2π; in this panel gray shaded regions indicate stable EFMs. Panel (b) shows a fundamental 2π-interval of C_p; in this panel white regions indicate one stable EFM, light gray regions two stable EFMs, and dark gray regions three stable EFMs.

feedback strength κ and the filter linewidth Λ, can have substantial influence on the multistable EFM regions [3,9]. Finally, we mention that bifurcating periodic solutions occur stable in large regions that give rise to an additional degree of multistability [10].

4. Conclusions

We studied the multistable continuous wave emission of a semiconductor laser subject to coherent optical feedback from a Fabry-Perot filter. Saddle-node bifurcations create an increasing number of external filtered modes as the laser frequency get close to the center frequency of the filter. The stability regions of those external filtered modes overlap which leads to multistability of between up to three external filtered modes. Here we concentrated on the stability of the external filtered modes. We found several codimension-two saddle-node Hopf, Bogdanov-Takens and double Hopf points that indicate a complex bifurcation structure of periodic orbits. For example, Refs. [3,10] contain a more comprehensive bifurcation analysis in dependence on different system parameters, which also includes the study of coexisting periodic orbits.

References

1. M. Yousefi and D. Lenstra, *IEEE Journal of Quantum Electronics* **35**, 970 (1999).
2. K. Green and B. Krauskopf, *Optics Communications* **258**, 243 (2006).
3. H. Erzgräber, B. Krauskopf and D. Lenstra, *SIAM Journal on Applied Dynamical Systems* **6**, 1 (2007).
4. A. P. A. Fischer, M. Yousefi, D. Lenstra, M. W. Carter and G. Vemuri, *Phys. Rev. Lett.* **92**, p. 023901 (2004).
5. G. Hek and V. Rottschafer, *IMA J Appl Math* **72**, 420 (2007).
6. V. Z. Tronciu, H.-J. Wünsche, M. Wolfrum and M. Radziunas, *Physical Review E* **73**, p. 046205 (2006).
7. T. Dahms, P. Hövel and E. Schöll, *Physical Review E* **78**, p. 056213 (2008).
8. K. Engelborghs, T. Luzyanina and G. Samaey, *DDE-BIFTOOL v. 2.00 user manual: a Matlab package for bifurcation analysis of delay differential equations.*, Technical Report TW-330, Department of Computer Science (K. U. Leuven, Leuven, 2001).
9. H. Erzgräber and B. Krauskopf, *Optits Letters* **32**, 2441 (2007).
10. H. Erzgräber, D. Lenstra, B. Krauskopf, A. P. A. Fischer and G. Vemuri, *Physical Review E* **76**, p. 026212 (2007).